AD_____

Award Number:

    W81XWH-04-1-0630

TITLE:

    Surface Enhanced Raman Spectroscopy for Monitoring Lactate
and Glucose

PRINCIPAL INVESTIGATOR:

    Matthew Glucksberg, Ph.D.

CONTRACTING ORGANIZATION:
    Northwestern University
    Evanston, IL 60202

REPORT DATE:

    July 2006

TYPE OF REPORT:

    Final

PREPARED FOR: U.S. Army Medical Research and Materiel Command
               Fort Detrick, Maryland 21702-5012

DISTRIBUTION STATEMENT:

    Approved for public release; distribution unlimited

REPORT DOCUMENTATION PAGE

1. REPORT DATE *(DD-MM-YYYY)*	2. REPORT TYPE	3. DATES COVERED *(From - To)*
01-07-2006	Final Report	01 Jul 04 – 30 Jun 06

4. TITLE AND SUBTITLE

Surface enhanced Raman spectroscopy for monitoring lactate and glucose

5a. CONTRACT NUMBER

5b. GRANT NUMBER
W81XWH-04-1-0630

5c. PROGRAM ELEMENT NUMBER

6. AUTHOR(S)
Matthew Glucksberg, PhD
Joseph Walsh, PhD
Richard Van Duyne, PhD

5d. PROJECT NUMBER

5e. TASK NUMBER

5f. WORK UNIT NUMBER

7. PERFORMING ORGANIZATION NAME(S) AND ADDRESS(ES)

Northwestern University
633 Clark St
Evanston IL 60208

8. PERFORMING ORGANIZATION REPORT NUMBER

9. SPONSORING / MONITORING AGENCY NAME(S) AND ADDRESS(ES)

USAMRMC
504 SCOTT STREET
FORT DETRICK, MD 21702-5012

10. SPONSOR/MONITOR'S ACRONYM(S)

11. SPONSOR/MONITOR'S REPORT NUMBER(S)

12. DISTRIBUTION / AVAILABILITY STATEMENT

Approved for public release; distribution unlimited

13. SUPPLEMENTARY NOTES

14. ABSTRACT
The development of a robust, portable, and simple biomedical device for the monitoring of glucose, lactate and other metabolites of interest is of great practical importance to routine treatment of diabetes and to the evaluation of individuals under high-stress situations, e.g. warfighters and astronauts. Raman spectroscopy is a powerful analytical tool that permits the unambiguous identification of molecules based on their unique vibrational modes. This spectral fingerprinting of molecules is well suited to multi-analyte detection without cumbersome sample preparation or separation. The Surface Enhanced Raman Scattering (SERS) phenomenon increases by up to a trillion fold the Raman signal from molecules near gold and silver nanoscale materials. We have shown that the incorporation of chemically tailored coatings on SERS active surfaces may serve as a partitioning layer, selectively concentrating the molecules of interest near the surface, thus simultaneously increasing target signal and decreasing the noise signal from interferants even with very low power (~1mW) lasers. We have successfully developed and tested these SERS active substrates in vitro and in vivo in the subcutaneous space of a rat. Work continues in rat models of hyperglycemia and hyperlactatemia.

15. SUBJECT TERMS

Raman spectroscopy, metabolite monitoring

16. SECURITY CLASSIFICATION OF:			17. LIMITATION OF ABSTRACT	18. NUMBER OF PAGES	19a. NAME OF RESPONSIBLE PERSON USAMRMC
a. REPORT U	**b. ABSTRACT** U	**c. THIS PAGE** U	UU	12	**19b. TELEPHONE NUMBER** *(include area code)*

Table of Contents

INTRODUCTION

The overall project goal is to demonstrate a sensor based on surface-enhanced Raman spectroscopy (SERS) that measures glucose and lactate. We have successfully demonstrated feasibility of using this system for detection *in vitro* and *in vivo* as specified in the original proposal.

The specific aims, as proposed in the original "statement of work" included:

Task 1. To develop and optimize SERS (Surface Enhanced Raman Active) surfaces and partition layers for the detection of glucose and lactate, *in vitro*.

    a. Determine optimal nanoscale geometry for SERS-active substrate.
    b. Optimize, *in vitro*, partition layers for best selectivity to target molecules glucose and lactate.
    c. Test effectiveness of probe configurations.

Task 2. Use a rat model to monitor analyte concentrations and assess performance.

    a. Control experiments.
    b. Use indwelling probes to quantitatively measure glucose levels *in vivo*.
    c. Use indwelling probes to quantitatively measure lactate levels *in vivo*.
    d. Use indwelling probes to quantitatively measure lactate and glucose levels *in vivo*.
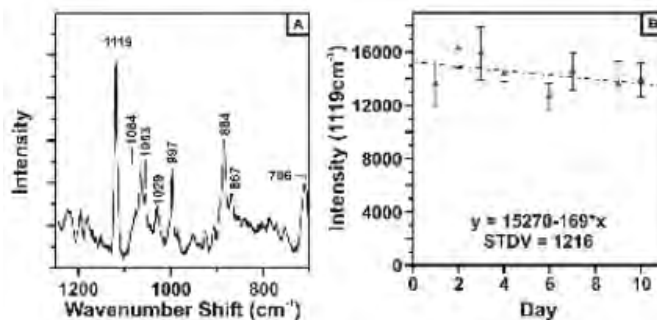
At present, 14 publications [1-14] and one patent [15] have either appeared in the literature or are in press. We demonstrated the following: (1) long term stability of the DT/MH-functionalized AgFON surface, (2) reversibility of the sensor for varying glucose and lactate concentrations, (3) quantitative measurement of glucose and lactate, and (4) rapid partitioning/departitioning time constants following a step change in concentration. Furthermore, we demonstrated (5) quantitative measurements of glucose at physiologic concentrations *in vivo* in a rat model with an implantable sensor. In an effort to improve the mechanical stability and explore alternative SERS-active substrates, we have (6) shown that anchored nanoparticle arrays are able to withstand 3 times the normal force compared to metal particles on flat glass surfaces.

Stability: DT/MH-functionalized AgFON surfaces are 10 days in bovine plasma (**Figure 4**). SER spectra were captured every 24 hours from three different samples and three spots on each sample (λ_{ex} = 785 nm, t = 2 min). **Figure 4A** represents the DT/MH spectrum acquired on day 2. **Figure 4B** shows the average intensity of the 1119 cm^{-1} peak for DT/MH on the AgFON for each day as a function of time. The 1119 cm^{-1} band corresponds to a symmetric stretching vibration of a C–C bond. The change in intensity of the 1119 cm^{-1} peak from the first day to the last day is 2.08%, indicating that the SAM was stable during the ten day period. This 2% change in intensity can be attributed to the rearrangement of the SAM during the incubation in bovine plasma. The temporal stability of the 1119 cm^{-1} peak intensity indicates that the DT/MH SAM is intact and well ordered, making this SAM-functionalized surface a potential candidate for an implantable sensor.

Reversibility – Glucose: An implantable glucose sensor must be reversible in order to successfully monitor fluctuations in glucose concentration throughout the day. To demonstrate the reversibility of the sensor, the DT/MH-modified AgFON sensor was exposed to cycles of 0 and 100 mM aqueous glucose solutions (pH ~ 7) without flushing the sensor between measurements in order to simulate real-time sensing (**Figure 5 inset**). Nitrate was used as an internal standard in all the experiments (1053 cm^{-1} peak) to minimize the effect of any laser power fluctuations. The 1053 cm^{-1} band corresponds to a symmetric stretching vibration of NO$_3^-$ and was used to normalize the spectra. SER spectra were collected following each step change in glucose concentration (λ_{ex} = 532 nm, P = 10 mW, t = 20 min) (**Figure 5A, 5B, 5C, 5D**). **Figure 5E** shows the normal Raman spectrum of a saturated aqueous glucose solution for comparison. In the normal Raman spectrum of a saturated aqueous glucose solution, peaks at 1462, 1365, 1268, 1126, 915, and 850 cm^{-1} correspond

Figure 5: Inset shows the step changes in glucose concentration experienced by the sensor. (A, B, C, D) SER spectra collected for each step. (E) Normal Raman spectrum of saturated aqueous glucose solution. (F, G, H, I) Differences indicating glucose partitioning and departitioning. Raman bands in the difference spectra showing glucose (F, G) agree well with the reference glucose spectrum (E). a.d.u. denotes analog-to-digital converter units mW^{-1} sec^{-1}.

to crystalline glucose peaks. The difference spectra found by subtracting low concentration steps from high concentration steps (**spectra B – A, D – C, Figure 5F, 5G**) represent partitioning of glucose in the DT/MH SAM, which clearly show the glucose features at 1461, 1371, 1269, 1131, 916, and 864 cm^{-1}. These correspond to the peaks in the normal Raman spectrum of glucose in aqueous solution (**Figure 5E**). We should note that the literature has shown that SERS bands can shift up to 25 cm^{-1} when compared to normal Raman bands of the same analyte. The sharp peak seen in all of the difference spectra at 1053 cm^{-1} represents imperfect subtraction of the nitrate internal standard. The absence of glucose spectral features in the difference spectra found by subtracting low concentration steps from each other and high concentration steps from each other (**spectra C – A, D – B, Figure 5H, 5I**) indicates complete departitioning of glucose. **The DT/MH mixed SAM presents a completely reversible sensing surface for optimal partitioning and departitioning of glucose.**

Reversibility – Lactate: To demonstrate proof-of-concept that this sensor could eventually be used for sensing other important analytes, we have also used the DT/MH SAM to detect lactate in physiological concentrations. To demonstrate the reversibility of the sensor, the DT/MH-modified AgFON sensor was exposed to cycles of 0 and 100 mM aqueous lactate solutions (pH ~ 5) without flushing the sensor in between measurements in order to simulate real-time sensing (**Figure 6 inset**). SER spectra were collected for each step change in concentration (λ_{ex} = 532 nm, P = 10 mW, t = 20 min) (**Figure 6A, 6B, 6C, 6D**). **Figure 6E** shows the normal Raman spectrum of a saturated aqueous lactate solution for comparison. In the normal Raman spectrum of a 0.8 M aqueous lactate solution, peaks at 1457, 1420, 1368, 1321, 1276, 1127, 1090, 1048, 934, and 866 cm^{-1} correspond to aqueous lactate ion peaks. The difference spectra (**Figure 6F, 6G**) represent partitioning of lactate in DT/MH SAM, which clearly show the lactate
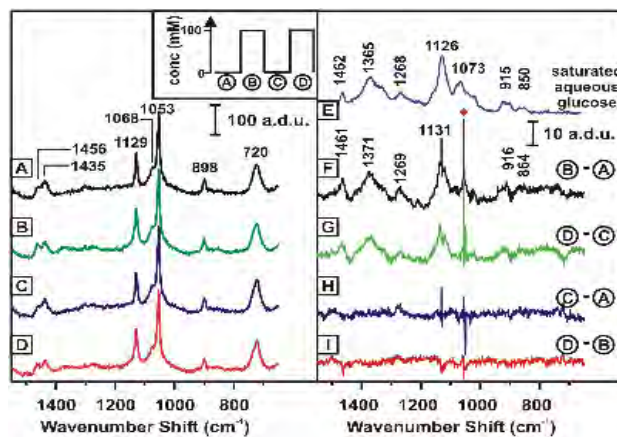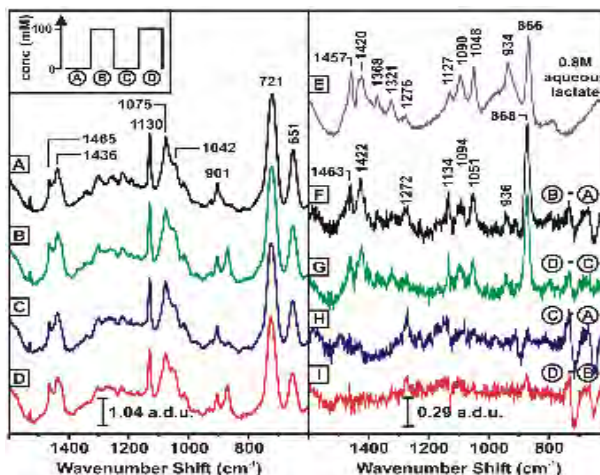
Figure 6:
Inset shows the step changes in lactate concentration experienced by the sensor. (A, B, C, D) SER spectra collected for each step. (E) Normal Raman spectrum of 0.8 M aqueous lactate solution. (F, G, H, I) Differences indicating lactate partitioning and departitioning. Raman bands in the difference spectra showing lactate (F, G) agree well with the reference lactate spectrum (E). a.d.u. denotes analog-to-digital units mW^{-1} sec^{-1}.

features at 1463, 1422, 1272, 1134, 1094, 1051, 936, and 868 cm^{-1}. These features correspond to the peaks in the normal Raman spectrum of lactate in aqueous solution (**Figure 6E**). The absence of lactate spectral features in the difference spectra (**Figure 6H, 6I**) represents complete departitioning of lactate. **The DT/MH mixed SAM is a completely reversible sensing surface for optimal partitioning and departitioning of lactate.**

Quantitative glucose detection: In order for a glucose sensor to be viable, it must be able to detect glucose in the clinically relevant range 10-450 mg/dL (0.56-25 mM), at physiological pH, and in the presence of interfering analytes (**Figure 7**). The data are presented in the Clarke error grid, a standard for evaluating the reliability of glucose sensors in the clinically relevant concentration range (0-450 mg/dL). Data that fall in the A and B range are acceptable values. Values outside the A and B range are poorly quantified and can lead to erroneous diagnosis and treatment. DT/MH-functionalized AgFON samples were placed in a flow cell containing water (pH ~ 7) with potential interferents lactate (1 mM) and urea (2.5 mM) in physiological concentrations. Glucose solutions ranging from 10 to 450 mg/dL were then randomly introduced in the cell and incubated for 2 min to ensure complete partitioning. SER spectra were collected using two substrates and multiple spots on each substrate
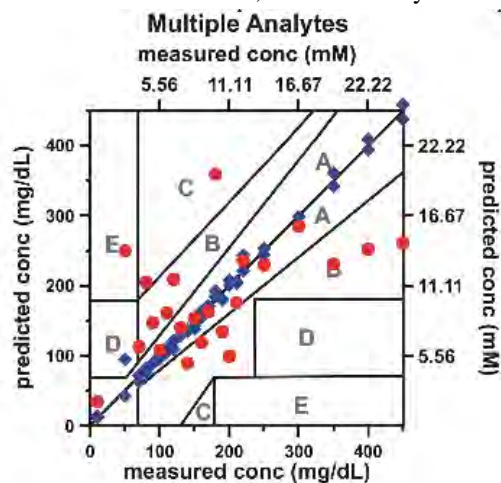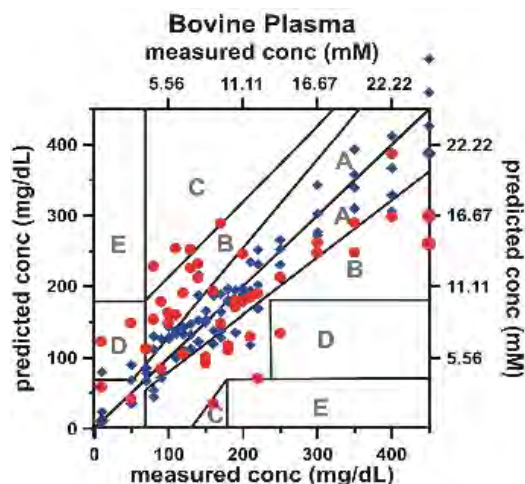
Figure 7: Glucose calibration (diamonds) and validation (circles) plot using two substrates and multiple spots. PLS calibration plot was constructed using 46 data points and validation plot was constructed using 23 data points taken over a range of glucose concentrations (10 - 450 mg/dL) in 1 mM lactic acid and 2.5 mM urea at pH ~7. RMSEC = 9.89 mg/dL (0.55 mM) and RMSEP = 92.17 mg/dL (5.12 mM) with 7 loading vectors. λ_{ex}= 785 nm, P = 8.4 mW, t = 2 min.

using a near-infrared laser source (λ_{ex} = 785 nm, P = 8.4 mW, t = 2 min). A calibration model was constructed using partial least squares leave-one-out (PLS-LOO) analysis with 46 randomly chosen independent spectral measurements of known glucose concentrations. The calibration model was based upon 7 latent variables which take into account variation in laser power, the environment in the lab, and SERS enhancement at different locations. The PLS analysis yields a root mean square error of calibration (RMSEC) of 9.89 mg/dL (0.549 mM). This RMSEC value is lower than that reported in our previous work using the EG3-modified AgFON.

In addition to having a low RMSEC, it is important to use an independent validation set to test the calibration model. For this experiment, a set of 23 data points was used to validate the model. The root mean square error of prediction (RMSEP) was calculated to be 92.17 mg/dL (5.12 mM). **Figure 7 shows that 98% of the calibration points and 87% of the validation points fall in the A and B range of the Clarke error grid.** To transition from the *in vitro* sensor to an *in vivo* sensor, the sensor should also demonstrate quantitative detection in a more complex medium. Bovine plasma was used to simulate the *in vivo* environment of an implantable glucose sensor. Prior to use, bovine plasma was filtered using a 0.45 µm diameter pore size filter. The filtered plasma was then spiked with glucose concentrations ranging from 10-450 mg/dL. DT/MH-functionalized AgFON substrates were placed in the flow cell and exposed to the glucose spiked bovine plasma. SER spectra were collected at each concentration using multiple samples and multiple spots in random order to construct a robust calibration model (λ_{ex} = 785 nm, P = 10-30 mW, t = 2 min). Calibration was constructed using the PLS-LOO analysis described above using 7 latent variables and presented in a Clarke error grid (**Figure 8**). To construct the calibration, 92 randomly chosen data points were used, resulting in an RMSEC of 34.3 mg/dL (1.90 mM). For the validation, 46 data points were used with an RMSEP of 83.16 mg/dL (4.62 mM). **In the Clarke error grid, 98% of the calibration points and 85% of the validation points fall in the A and B range.** Error can be attributed to variation in SERS enhancement at different spots and different substrates. The errors in both experiments can be reduced by using more data points for the calibration. **The results show that the DT/MH-modified AgFON glucose sensor is capable of making accurate glucose measurements in the presence of many interfering analytes.**

Quantitative lactate detection: As stated previously, we have also done some experiments as proof-of-concept that this sensor can eventually be used for other analytes. We demonstrate quantitative lactate detection in the clinically relevant range 6-240 mg/dL (0.5-22 mM), in a simple aqueous system, and in the system buffered with phosphate buffered saline (PBS) (**Figure 9, Figure 10**). DT/MH-functionalized AgFON samples were placed in a flow cell and lactate solutions ranging from 6 to 240 mg/dL were randomly introduced in the cell and incubated for 2 min to ensure complete partitioning. SER spectra were collected using multiple spots with a visible laser source (λ_{ex} = 532 nm, P = 7.5 - 12 mW, t = 2 min). Calibration models were constructed using partial least squares leave-one-out (PLS-LOO) analysis with 48 to 50 randomly chosen independent spectral measurements of known lactate concentrations. The calibration models were based upon 7 latent variables that take into account variation in laser power, the environment in the lab, and SERS enhancement at different locations. The PLS analysis results in a root mean square error of calibration (RMSEC) of 21.64 mg/dL (2 mM) for the water system and an RMSEC of 17.8 mg/dL (1.6 mM) for the buffered system.

Figure 8: Glucose calibration (diamonds) and validation (circles) plot using three substrates and multiple spots acquired in two days. PLS calibration plot was constructed using 92 data points and validation plot was constructed using 46 data points taken over a range of glucose concentrations (10 - 450 mg/dL) in bovine plasma. RMSEC = 34.3 mg/dL (1.9 mM) and RMSEP = 83.16 mg/dL (4.62 mM) with 7 loading vectors. λ_{ex} = 785nm, P = 10-30 mW, t = 2 min.

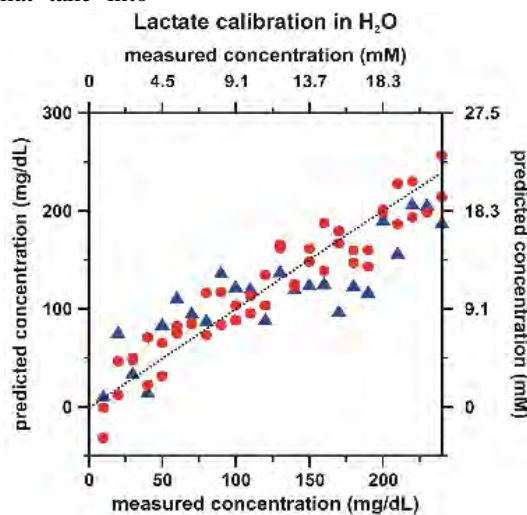**Figure 9:** Lactate calibration (circles) and validation (diamonds) plot using multiple spots on a single substrate in water. PLS calibration plot was constructed using 48 data points and validation plot was constructed using 24 data points taken over a range of lactate concentrations (10 - 240 mg/dL). RMSEC = 21.64 mg/dL (2 mM) and RMSEP = 37.58 mg/dL (3.4 mM) with 7 loading vectors. λ_{ex} = 532 nm, P = 7-12 mW, t = 2 min.

For validation of the models for lactate, sets of 24 to 25 independent data points were used. The root mean square error of prediction (RMSEP) was calculated to be 37.58 mg/dL (3.4 mM) for the aqueous system and 39.6 mg/dL (3.6 mM) for the PBS system. The RMSEP can be improved by increasing the number of data points in the calibration set. These data reflect an initial attempt to quantify lactate concentration using SERS. **The data demonstrate the feasibility of lactate measurements,** but also makes apparent the need for further optimization of the sensing platform to improve the detection limits and reduce prediction errors. The main feature of the sensor that will aid in sensitivity and selectivity of the sensor is the partition layer on the SERS-active surface, which will be discussed in the Research Design section in detail.

Real-time partitioning and departitioning of glucose and lactate: In addition to reversibility, which is an important characteristic for a viable sensor, the sensor should be able to partition and departition the analyte of interest on a reasonable time scale. The real-time response for glucose was examined in a system with bovine plasma simulating the *in vivo* environment, while for lactate, the measurements have been performed in a water system. To evaluate the real-time response of the sensor, the $1/e$ time constant for partitioning and departitioning was calculated.

In the case of glucose, a DT/MH-functionalized AgFON was placed in bovine plasma for 5 h. The AgFON surface was then placed in a flow cell. SER spectra were collected continuously (λ_{ex} = 785 nm P = 10 mW) with a 15-s integration time. To observe
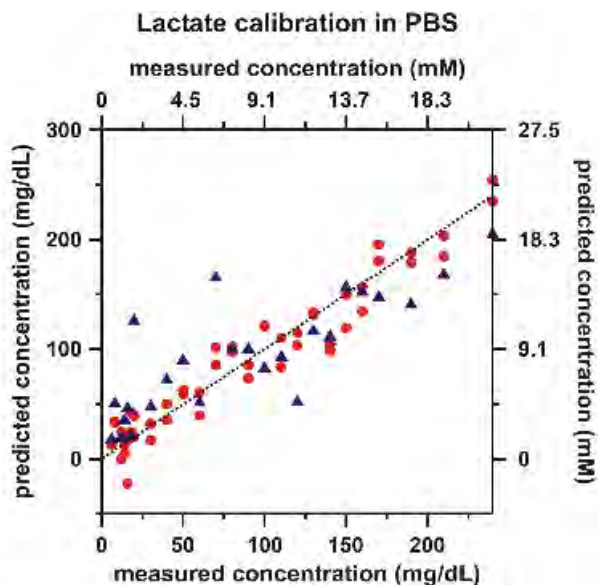

Figure 10: Lactate calibration (circles) and validation (diamonds) plot using multiple spots on a single substrate in phosphate buffered saline (PBS). PLS calibration plot was constructed using 50 data points and validation plot was constructed using 25 data points taken over a range of lactate concentrations (6 - 240 mg/dL). RMSEC = 17.8 mg/dL (1.6 mM) and RMSEP = 39.6 mg/dL (3.6 mM) with 7 loading vectors. λ_{ex} = 532 nm, P = 7-12 mW, t = 2 min.

partitioning, 50 mM glucose solution in bovine plasma was injected at t = 0. At t = 225 s, 0 mM glucose solution in bovine plasma was injected into the flow cell to evaluate the departitioning of glucose. An excitation wavelength of 785 nm was used to reduce autofluorescence caused by proteins. The amplitude was then plotted versus time as shown in **Figure 11C**. The $1/e$ time constant was calculated from an exponential curve fit to the data. The spectra shown in **Figure 11A** and **11B** demonstrate real-time amplitude changes in the 1462-cm[-1] peak as the glucose concentration varies. The amplitude of the 1462-cm[-1] peak was obtained by fitting the data to the superposition of three Lorentzian line shapes using PeakFit. The $1/e$ time constant is 28 s for partitioning and 25 s for departitioning, calculated from the exponential fit (**Figure 11C**). **These experiments demonstrate that partitioning and departitioning occur rapidly making the SERS-based glucose sensor a potential candidate for implantable, continuous sensing.**

For lactate, the $1/e$ time constant was obtained in a similar manner. A DT/MH-functionalized AgFON was mounted in a flow cell which was then filled with water. SER spectra were collected continuously for 10 minutes with 15-s integration time for each frame at an excitation wavelength of 532 nm. To observe partitioning, 100 mM aqueous lactate solution was injected at t = 0. At t = 315 s, 0 mM lactate solution was rapidly injected into the flow cell to observe departitioning. The partitioning dynamics of lactate were evaluated by examining the intensity of the C—COO[-] vibrational stretch of lactate at 860 cm^{-1}. The time constant was determined by fitting an exponential curve to **the data**. The calculated $1/e$ time constant was 1.2 s for partitioning and 1 s for departitioning of lactate.
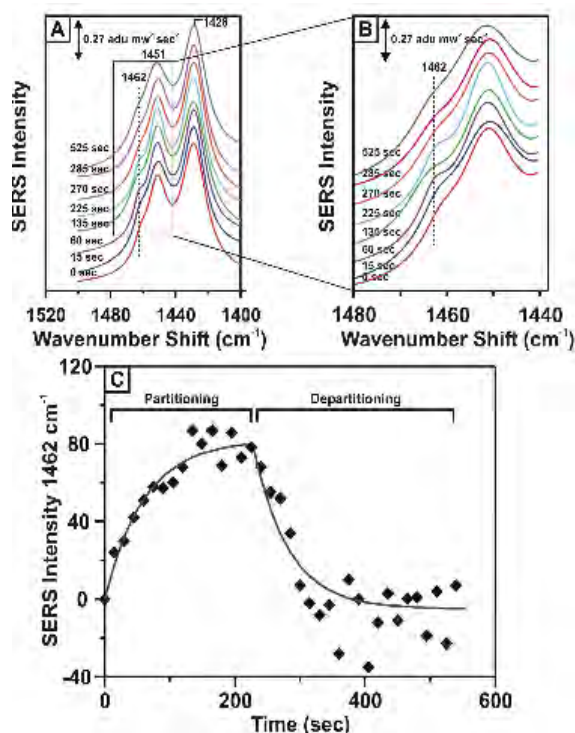

Figure 11: Real-time SERS response to a step change in glucose concentration in bovine plasma. (A) SER spectra of the SAM and glucose at various times. Peaks at 1451 and 1428 cm^{-1} are features of SAM and 1462 cm^{-1} indicates glucose. Glucose was injected at t = 0 s, and the cell was flushed with bovine plasma at t = 225 s. (B) Expanded scale version of (A) from 1480 to 1440 cm^{-1}. (C) Partitioning and departitioning of glucose. λ_{ex} = 785 nm, P_{laser} = 100 mW, and t = 15 s. The 1/e time constants were calculated to be 28 s for partitioning and 25 s for departitioning.
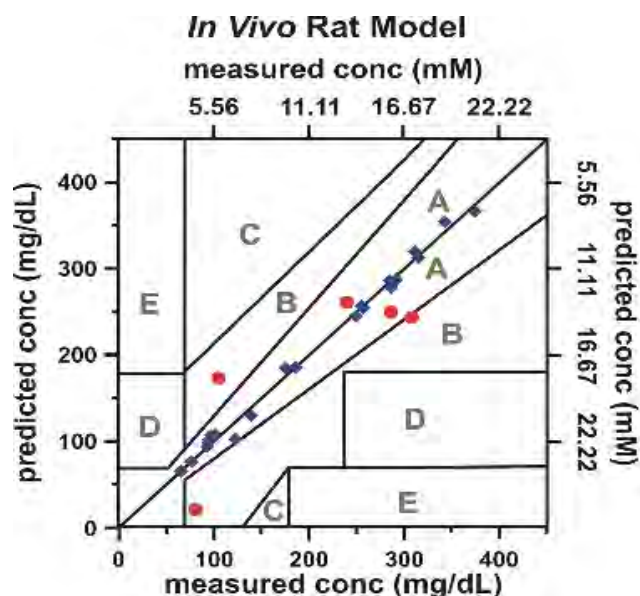
Figure 12: Glucose calibration (diamonds) and validation (circles) plot using a single substrate and a single spot on a DTMH functionalized AgFON on a mesh. PLS calibration plot was constructed using 21 data points and validation plot was constructed using 5 data points taken over a range of glucose concentrations (10 - 450 mg/dL) *in vivo* (rat). RMSEC = 7.46 mg/dL (0.41 mM) and RMSEP = 53.42 mg/dL (2.97 mM). λ_{ex}=785nm, P = 50 mW, t = 2 min.
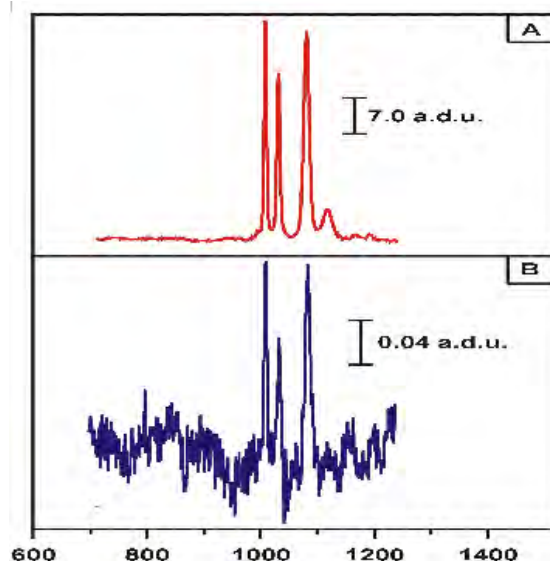
Figure 13: Transdermal measurement of benzenethiol on AgFON. (A) shows the SERS spectra of benzenethiol directly on AgFON. (λ_{max} = 785 nm, P = 47.5 mW, t = 60 sec). (B) shows the transdermal SERS spectra of benzenethiol on AgFON. The signal intensity is 100 times weaker than in (A) (λ_{max} = 785 nm, P = 275 mW, t = 20 sec). a.d.u. denotes analog-to-digital units mW^{-1} sec^{-1}.

***In vivo* glucose detection:** We have demonstrated successful detection of glucose *in vivo* with an implantable SERS sensor using a rat animal model. A Sprague-Dawley rat was weighed and anesthetized with pentobarbital (Ovation Pharmaceuticals, Inc.) using a dose of 50 mg/kg. Then, the femoral vein was cannulated using PE 50 tubing (Clay Adams) for glucose injections and the carotid artery was cannulated using PE 90 tubing for blood glucose measurements with a commercially available glucometer (One Touch II blood glucose meter). The incisions were shut with surgical clips. Every hour, the rat was given an additional half dose of the anesthetic. Throughout the experiment the rat was warmed with an electric heating pad. The rat was also attached to a ventilator to aid breathing. To collect SER spectra, a metal frame containing a glass window was placed along the midline of the rat's back.

A DT/MH functionalized AgFON surface supported on a Cu mesh was positioned between the skin and the window such that the substrate was in contact with the interstitial fluid. An aliquot of glucose (1 g/mL in saline) was injected in the rat to artificially vary the blood glucose level. An aliquot of blood was drawn from the rat to measure the blood glucose level using the One Touch II blood glucose meter. SER spectra were acquired through the window using a Ti:Sapphire laser (λ_{ex} = 785 nm, P = 50 mW, time = 2 min). The SER spectra showed a pronounced Raman band characteristic of the SAM (data not shown). Additional bands were observed compared to the spectra collected in the bovine plasma model; however, the Raman bands were not obscured by autofluorescence because near infra-red excitation was used. All SER spectra were analyzed using PLS-LOO and represented on the Clarke error grid. In **Figure 12**, 21 data points were used to build the calibration model and five data points were used to validate the model. All the data points in both calibration and validation fall in A and B range of the Clarke error grid with the RMSEC = 7.46 mg/dL and RMSEP = 53.42 mg/dL.

The glucose level was artificially varied in the rat through intravenous injection for three hours. An aliquot of blood was drawn from the rat and glucose level was checked with the One Touch II blood glucose meter and corresponding SERS measurements were taken.

Transdermal measurement: In order to transition the SERS based glucose sensor for *in vivo* measurements it is important to focus on the design of the sensor. There are several different modalities that can be explored including the use of fiber optic probes and direct transdermal measurements. As a proof-of-principle experiment for transdermal measurements, we have taken SERS spectra of benzenethiol through rat skin. **Figure 13** shows the SERS measurement of benzenethiol on an AgFON directly (**Figure 15A**) and transdermally (**Figure 13B**). The intensity of the transdermal measurement results in a 100 times weaker signal than direct measurement on an AgFON. Data was collected with a 785 nm laser with the following parameters: for **Figure 15A** t= 60 sec, P = 47.5 mW; for **Figure 13B** t = 20 sec, P = 275 mW .

Particles anchored in nanowells: In parallel with the development and optimization of the AgFON SERS-active substrates, we have been exploring other nanosphere lithography (NSL) based SERS-active substrates. Well-ordered tetrahedral nanoparticle arrays present highly sensitive SERS-active substrates due to their strongly enhanced localized electromagnetic fields and tunable optical

properties. However, metal nanoparticle arrays fabricated on glass substrates suffer from inferior stability due to the weak adhesion between metal and SiO$_2$ in an aqueous environment.

Particles anchored in nanowells, in addition to the extra degree of freedom in the tunability of optical properties, provide a more robust, mechanically stable substrate for sensor applications. Nanowells are fabricated through the polystyrene sphere mask by reactive ion etching (RIE). Adhesion of the nanoparticles to the surface was examined by atomic force microscopy (AFM) normal force measurements as shown in the schematic in **Figure 14**. Normal force applied by the AFM cantilever can be calculated by

$$F = k \cdot DS \cdot z$$

where k is the spring constant of the cantilever (0.187 N/m), DS is the detector sensitivity reported in the units of nm/V (0.833), and z is the deflection of the cantilever given in volts. Normal force, although not a direct measure of adhesion, gives a qualitative characteristic of the nanoparticles' stability. It is the force applied by the cantilever as it scans the surface of the substrate. The normal force is proportional to the deflection of the cantilever. The normal force needed to remove metal nanoparticles from an unetched glass surface was determined for comparison. The nanoparticles were fabricated using a 510 nm nanosphere mask. The resulting particles had an out-of-plane height of 55 nm Ag. A 100 μm^2 area of the substrate was scanned using contact mode AFM with incrementally increasing deflection setpoint from -2 V to 0.5 V. Most of the nanoparticles were removed at a setpoint of 0.5 V, which is equivalent to a normal force of 12.39 nN. Moving nanoparticles are characterized on the image by the trail left behind after being dragged by the tip (**Figure 14**). The normal force calculated agrees with previously reported normal force measurements needed to displace metal nanoparticles.

Anchored nanoparticle substrates were examined in the same manner. The anchored nanoparticles were fabricated using a 510 nm sphere mask with a 3 min etch at 25 W, and 55 nm of Ag was deposited. The nanoparticles were embedded into a well 10 – 15 nm deep. Contact force AFM scans over a 100 μm^2 area were acquired with incrementally increasing deflection setpoints. Most of the nanoparticles were removed at a deflection setpoint of 9 V (35.08 nN). **These results indicate that the anchored nanoparticles provide a more robust surface for sensors than nanoparticle arrays on flat glass surfaces.** Anchored nanoparticles demonstrate a 3-fold improvement in mechanical stability of the surface. This increase in mechanical stability allows the anchored nanoparticle arrays to be placed in harsh environments where traditional arrays would become damaged or delaminated.

Fiber optic measurements: The feasibility of fiber-optic detection is demonstrated using a bifurcated fiber probe with one excitation and one collection fiber. First, benzenethiol, a strong Raman scatterer, was used as a target molecule. A collimating lens was used at the collection side of the fiber probe to improve the collection efficiency. The edge of the lens was placed 2-3 mm from the surface of the AuFON at an approximate angle of 5 degrees from normal incidence.

Figure 14: Top panel: schematic of the normal atomic force experiment. The particle can be moved by the cantilever when adhesion is weak. Bottom panel: contact atomic force micrograph of the nanoparticle array on a flat surface. The nanoparticles at the top of the image remain intact at low deflection setpoints while most nanoparticles in the bottom section have been removed with increasing applied force.

A SERS spectrum of benzenethiol is shown in **Figure 15A**. The inset shows the spectrum on the same sample acquired in air without any fiber optic components. The signal obtained through the fiber clearly matches the reference spectrum with both showing the peaks at 1076 cm^{-1}, 1024 cm^{-1}, and 1000 cm^{-1}. SERS spectra of EG3 using the fiber optic probe and in air (inset) are shown in **Figure 15B**. Raman bands of EG3 at 1079 cm^{-1}, 1031 cm^{-1}, 889 cm^{-1}, and 702 cm^{-1} match closely the bands on the EG3 spectrum acquired without

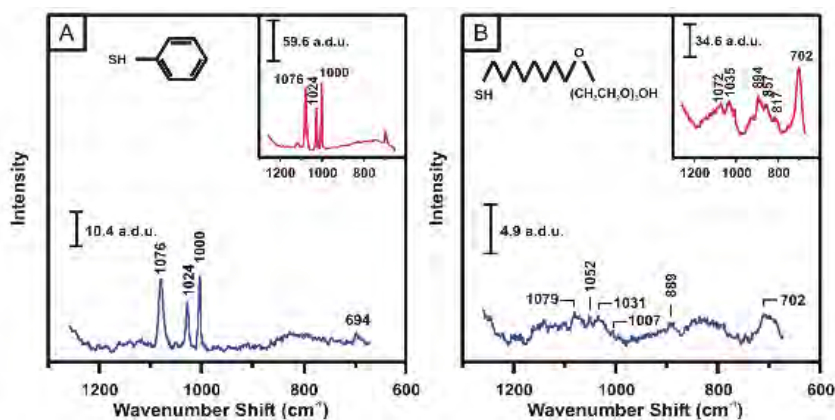**Figure 15:** SERS spectra of (A) benzenethiol on AuFON and (B) EG3 on AgFON through a dual fiber probe, where one fiber was used for excitation and the other one was used for collection of scattered light. The insets show the comparative SERS spectra acquired on the same samples using a regular Raman setup with no fiber optic components. a.d.u. denotes analog-to-digital units electrons mW^{-1} sec^{-1}

fiber optic components. This demonstrates the feasibility of using the fiber optic probe for detection.

To determine the signal loss, the intensities of the 1000 cm^{-1} and 702 cm^{-1} peaks are examined in benezethiol and EG3, respectively. The raw intensity counts are normalized to the power and acquisition time, such that the intensity is reported in the units of electrons*mW^{-1}*sec^{-1} or analog-to-digital units (a.d.u.).(ref McCreery) The intensity of benzenethiol in air, I_{air}=190.5 a.d.u., while I_{fiber}=10.4 a.d.u. The signal is decreased by a factor of 20. In the case of EG3, I_{air}=54.2 a.d.u. and I_{fiber}=1.7 a.d.u., so the decrease is by a factor of 33.

Publications

1. Shah, N. C.; Lyandres, O.; Walsh, J. T., Jr.; Glucksberg, M. R.; Van Duyne, R. P. *Analytical Chemistry* 2007, *79*, 6927-6932.
2. Dieringer, J. A.; McFarland, A. D.; Shah, N. C.; Stuart, D. A.; Whitney, A. V.; Yonzon, C. R.; Young, M. A.; Zhang, X.; Van Duyne, R. P. *Faraday Discussions* 2006, *132*, 9-26.
3. Shafer-Peltier, K. E.; Haynes, C. L.; Glucksberg, M. R.; Van Duyne, R. P. *Journal of the American Chemical Society* 2003, *125*, 588-593.
4. Yonzon, C. R.; Haynes, C. L.; Zhang, X. Y.; Walsh, J. T.; Van Duyne, R. P. *Analytical Chemistry* 2004, *76*, 78-85.
5. Young, M. A.; Stuart, D. A.; McFarland, A. D.; Lyandres, O.; Glucksberg, M. R.; Van Duyne, R.P. *Canadian Journal of Chemistry* 2004, *82*, 1435-1441.
6. Stuart, D. A.; Yonzon, C. R.; Zhang, X.; Lyandres, O.; Shah, N.; Glucksberg, M. R.; Walsh, J. T.; Van Duyne, R. P. *Analytical Chemistry* 2005, *77*, 4013-4019.
7. Zhang, X.; Shah, N. C.; Van Duyne, R. P. *Vibrational Spectroscopy* 2005.
8. onzon, C. R.; Lyandres, O.; Shah, N. C.; Dieringer, J. A.; Van Duyne, R. P. In *SurfaceEnhanced Raman Scattering -- Physics and Applications*; Kneipp, K., Moskovits, M., Kneipp, H., Eds.; Springer: New York, 2006; Vol. 103, pp 367-379.
9. Zhang, X.; Shah, N. C.; Van Duyne, R. P. *Vibrational Spectroscopy* 2006, *42*, 2-8.
10. Hicks, E. M.; Lyandres, O.; Hall, W. P.; Zou, S.; Glucksberg, M. R.; Van Duyne, R. P. *Journal of Physical Chemistry C* 2007, *111*, 4116-4124.
11. 139. Shah, N. C.; Lyandres, O.; Yonzon, C. R.; Zhang, X.; Van Duyne, R. P. In *ACS Symposium Series*, 2007; Vol. 963, pp 107-122.
12. Lyandres, O.; Glucksberg, M. R.; Walsh, J. T.; Shah, N. C.; Yonzon, C. R.; Zhang, X.; Van Duyne, R. P., Eds. *Surface-Enhanced Raman Sensors for Metabolic Analytes*; John Wiley & Sons, Inc.: New York, 2008.
11. 141. Shah, N. C.; Yuen, J. M.; Glucksberg, M. R.; Walsh, J. T.; Van Duyne, R. P. In *In Vivo Analytical Chemistry of Glucose*; Stenken, J., Cunningham, D., Eds.; John Wiley & Sons, Inc.: New York, 2008, pp in press.
12. 142. Stiles, P. L.; Dieringer, J. A.; Shah, N. C.; Van Duyne, R. P. *Annual Reviews of Analytical Chemistry* 2008, *1*, in press.
13. 143. Yuen, J.; Lyandres, O.; Shah, N. C.; Van Duyne, R. P.; Walsh, J., J. T.; Glucksberg, M. R. *Diabetes Technol. Ther.* 2008, in press.
14. 144. Anker, J. N.; Hall, W. P.; Zhao, J.; Shah, N. C.; Van Duyne, R. P. *Nature Materials* 2008, in press.
15. 145. Van Duyne, R. P.; Glucksberg, M. R.; Shafer-Peltier, K.; Haynes, C. L.; Walsh, J.; (Northwestern University, USA). Application: US US, 2004, pp 33 pp.

U.S. Army Medical Research and Materiel Command Animal Use Report

Facility Name: _Northwestern University BME Dept_   Principal Investigator: _____
Address: _2145 Sheridan Rd Rm E310_____   (Signature)
                _Evanston, IL 60208_____   Principal Investigator: _Matt Glucksberg_____
                _____   (Typed/Printed Name)

                                                        E-mail Address: ___m-glucksberg@northwestern.edu___
Contract Number: US ARMY MRMC
          AWARD NUMBER 0410630   Phone Number: __847-491-7121_____
                                                        Fax Number: ____847-491-4928_____

This Report is for <u>Fiscal Year 2005</u> (01 October 2004 - 30 September 2005)

Definitions of Column Headings on Back of Form					
A. Animal	B. Number of animals purchased, bred, or housed but **not** yet used	C. Number of animals used involving no pain or distress	D. Number of animals used in which appropriate anesthetic, analgesic, or tranquilizing drugs were used to alleviate pain	E. Number of animals used in which pain or distress was not alleviated	F. Total Number of Animals (Columns C+D+E)
Dogs					
Cats					
Guinea Pigs					
Hamsters					
Rabbits					
Non-human Primates					
Sheep					
Pigs					
Goats					
Horses					
Mice					
Rats	0	0	20	0	20
Fish					
List Others:					

*AAALAC - Association for the Assessment and Accreditation of Laboratory Animal Care International
Note: Northwestern University is AAALAC, International, accredited. Last site visit was in July 2005.

        PURPOSE: The purpose of this form is to gather data related to animal use for research,

development, testing, evaluation, clinical investigations, diagnostic procedures, and/or instructional programs conducted by or for the U.S. Army Medical Research and Materiel Command. This report is **NOT** to be used to report all animals used at your facility unless all work was conducted under contract with the U.S. Army Medical Research and Materiel Command. A separate form must be prepared for each award. This report is to cover one fiscal year (01 October - 30 September).

DEFINITIONS/INSTRUCTIONS:

Column A: List all animals used for the research, development, testing, evaluation, clinical investigations, diagnostic procedures, and/or instructional programs conducted. For the purpose of this report, an animal is defined as **any living nonhuman vertebrate**.

Column B: Refers to the purchase, breeding, or other acquisition of individual animals in the reporting fiscal year for assignment to a particular work unit or protocol. Animals carried over from the previous fiscal year and not yet used in any procedures or studies, must be included in this number for the work unit or protocol to which they are assigned.

Column C: Number of animals used in which the procedures did not cause more than slight or momentary pain or distress.

Column D: Number of animals used that were given analgesics, anesthetics, or tranquilizers to relieve pain or distress.

Column E: Number of animals used in painful procedures in which pain relieving compounds were not administered.

Column F: Sum of columns C, D, and E.

Forward this report by DECEMBER 01 of each year to:

Commander
U.S. Army Medical Research and Materiel Command
ATTN: MCMR-ZB-PA
504 Scott Street
Fort Detrick, MD 21702-5012

Questions should be directed to the office above at 301-619-3776. Completed reports and/or questions may be faxed to this office at 301-619-4165.

NOTE: This report may be reproduced.